

# Effects of the Film Thickness on the Transient Conjugate Optical-thermal Fields in Thin Films Irradiated by Moving Sources in Back and Front Treatments

N.Bianco<sup>1</sup>, O.Manca<sup>\*2</sup>, S.Nardini<sup>2</sup> and D.Ricci<sup>2</sup>

<sup>1</sup>Dipartimento di Energetica, Termofluidodinamica applicata e Condizionamenti ambientali, Università degli Studi di Napoli Federico II, Piazzale Tecchio 80, 80125 Napoli, Italia

<sup>2</sup>Dipartimento di Ingegneria Aerospaziale e Meccanica, Seconda Università degli Studi di Napoli, via Roma 29, 81031 Aversa, Italia

\*Corresponding author: oronzio.manca@unina2.it

**Abstract:** A two dimensional instationary analysis of the conjugate optical-thermal fields induced in a multilayer thin film structure by a moving Gaussian laser source is carried out numerically in order to compare back and front laser treatment processes. The work-piece is considered semi-infinite along the motion direction and different thicknesses of the thin film are considered. Thermal and optical non-linearity is induced during transient heating, since the response of weakly absorbing thin films depends on temperature. The heat source can directly impinge the film surface or the glass substrate. The optical field is considered locally one dimensional and Maxwell equations are solved in order to evaluate the absorption in thin film while the thermal field is two dimensional. COMSOL Multiphysics 3.4 code has been adopted to solve this combined thermal and electromagnetic problem. Results are presented in terms of transient temperature profiles and fields for different Peclet numbers and a-Si thicknesses.

**Keywords:** Combined Heat Conduction and Radiation, Laser Source, Moving Sources, Thin Films, Manufacturing.

## 1. Introduction

Lasers provide extraordinary opportunities for innovation with an ever-widening range of material processing and manufacturing applications such as welding, cutting, heat treating of metals and manufacturing of electronic components [1]. Furthermore, the manufacturing of multilayer thin films deposited on glass substrate is accomplished by means of laser sources, too. The analysis of thermal

conductive and optical distributions is of paramount importance to broaden the fields of applications for manufacturing. Computational investigations of laser interactions with single and multilayer thin films on a glass substrate were carried out by Shah et al. [1] and Tanasawa et al. [2]. Grigoropoulos [3] investigated the dependence of the thermally optical non-linearity induced in multilayer thin films because they are functions of wavelength and temperature. Chen and Tien [4] analyzed the effects of temperature-dependent optical characteristics while the effects of anisotropic thermal properties were investigated by McGahan and Cole [5]. The conjugate optical and thermal fields in a multilayer thin film irradiated by a pulsed laser beam were analyzed in [6], where a first study on the transient behaviour of materials was accomplished. Bianco and Manca [7] extended the analysis presented in [7] to a two-dimensional problem. Nakano et al. [8] proposed a numerical model for a thin film structure, in which an absorbed laser power density with an exponential decay for each layer was considered in the thermal model. Bianco et al. [9] analyzed numerically the coupled optical-thermal field in a thin film on a glass substrate irradiated by a moving continuous laser source in quasi-steady state conditions for different Peclet numbers. Bianco et al. [10] and Avagliano et al. [11] investigated the conjugate optical-thermal fields induced by laser back-scribing processes and made a comparison with front treatment ones. A comparison between laser front and back treatment processing on thin films was carried out by Bianco et al. [12] for a semi-infinite work-piece. Temperature profiles and fields showed front laser treatment revealed lower temperatures and smaller heat affected zones.

In this paper, a numerical analysis of transient conjugate optical-thermal fields in thin films irradiated by a continuous Gaussian moving source in order to compare front and back treatment processes is carried out. The multilayer thin film (composed by an a-Si layer and a TCO one) is deposited on a glass substrate and it is irradiated by a Gaussian moving laser beam. Different Peclet numbers and a-Si thicknesses are considered. Since the optical and thermal fields are linked, this problem is solved by means of COMSOL Multiphysics 3.4.

Results are evaluated for a continuous moving laser source and they are presented in terms of temperature profiles and fields.

## 2. Mathematical Description

The investigated model is composed by an amorphous silicon layer thin film deposited over a TCO layer and a glass substrate (fig. 1). A Nd-YAG source is chosen and its wavelength is 1064 nm. The laser beam is continuous and it is characterized by a Gaussian distribution. It can irradiate the a-Si layer surface, in the front treatment process, or the substrate one, in the back treatment process, moving at constant velocities. The solid dimension along the motion direction is assumed to be as semi-infinite ( $L_x = 5$  mm), while finite thicknesses for TCO ( $s_t$ ) and a-Si layers ( $s_s$ ) are considered.

Thermal and optical properties are assumed as functions of temperature and the materials are considered isotropic. Thermal radiation is absorbed and absorption mechanism is modelled as a thermal generation as shown in the heat conduction equation. Radiative and convective heat losses from the surfaces toward the ambient are neglected and the thin film can be treated as a semitransparent material, due to its small thickness. In a coordinate system fixed to the heat source, according to the theory of moving heat source [13], a mathematical statement of the thermal conductive problem is:

$$\frac{\partial}{\partial x} \left( k_i(T) \frac{\partial T_i}{\partial x} \right) + \frac{\partial}{\partial z} \left( k_i(T) \frac{\partial T_i}{\partial z} \right) + \dot{u}^m(T_i, x, z) = \rho c \left( \frac{\partial T_i}{\partial \theta} - v \frac{\partial T_i}{\partial x} \right) \quad (1)$$

with  $i = f, t$  or  $s$  and for  $0 \leq x < L_x$ ,  $0 \leq z \leq s_f + s_t + s_s$ ,  $\theta > 0$ ; with  $s_f$  the thin film

thickness,  $s_t$  the TCO thickness and  $s_s$  the substrate thickness.

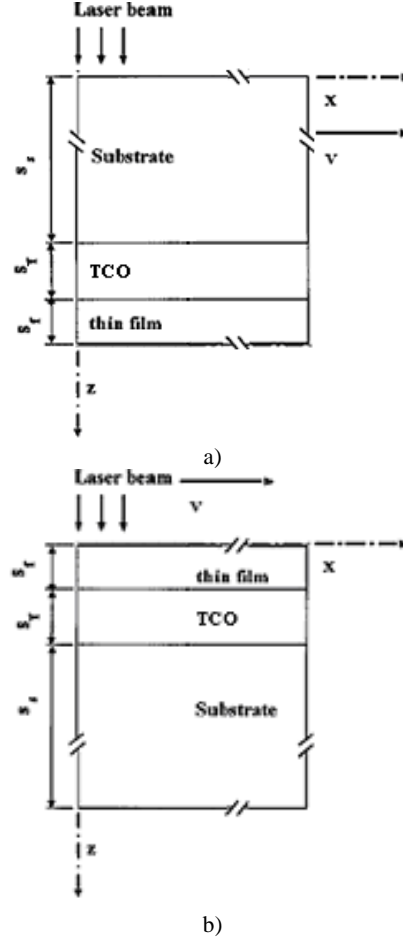


**Figure 1:** Sketch of the thin film and the TCO layer on glass substrate; a) front treatment; b) back treatment.

The boundary and initial conditions are reported in the following relations:

$$T_i(x, z, 0) = T_{in} \quad (2a)$$

with  $i=f, t$  or  $s$ , for  $0 \leq x < L_x$ ,  $0 \leq z \leq s_f + s_t + s_s$ ,

$\theta > 0$

$$-k_f \frac{\partial T_f(x, 0, \theta)}{\partial z} = 0 \quad (2b)$$

or for BT cases

$$-k_f \frac{\partial T_f(x, s_f + s_t + s_s, \theta)}{\partial z} = 0 \quad (2c)$$

for  $0 \leq x < L_x$ ,  $\theta > 0$

$$-k_s \frac{\partial T_s(x, s_f + s_t + s_s, \theta)}{\partial z} = 0 \quad (2d)$$

or for BT cases

$$-k_s \frac{\partial T_s(x,0,\theta)}{\partial z} = 0 \quad (2e)$$

for  $0 \leq x < L_x$ ,  $\theta > 0$

$$k_f \frac{\partial T_f(x,s_f,\theta)}{\partial z} = k_t \frac{\partial T_t(x,s_f,\theta)}{\partial z} \quad (2f)$$

or for BT cases

$$k_f \frac{\partial T_f(x,s_s+s_t,\theta)}{\partial z} = k_t \frac{\partial T_t(x,s_s+s_t,\theta)}{\partial z} \quad (2g)$$

for  $0 \leq x < L_x$ ,  $\theta > 0$

$$k_t \frac{\partial T_t(x,s_f+s_t,\theta)}{\partial z} = k_s \frac{\partial T_s(x,s_f+s_t,\theta)}{\partial z} \quad (2h)$$

or for BT cases

$$k_t \frac{\partial T_t(x,s_s,\theta)}{\partial z} = k_s \frac{\partial T_s(x,s_s,\theta)}{\partial z} \quad (2i)$$

for  $0 \leq x < L_x$ ,  $\theta > 0$

$$-k_t \frac{\partial T_t(0,z,\theta)}{\partial x} = 0 \quad (2f)$$

with i=f, t or s, for  $0 \leq z \leq s_f + s_t + s_s$ ,  $\theta > 0$

$$T_i(L_x,z,\theta) = T_{in} \quad (2g)$$

with i=f, t or s, for  $0 \leq z \leq s_f + s_t + s_s$ ,  $\theta > 0$

The generation term  $\dot{u}'''(T_i, x, z)$  is assumed as depending on optical material properties and is related to the Poynting vector S, by means of equation (4). The S evaluation is made by means of Maxwell equations and following the COMSOL indications:

$$S = \frac{n_a}{2\mu c'} |E_a|^2 \quad (3)$$

and the absorbed energy for unit volume:

$$\dot{u}'''(T_f, x, z) = -\frac{\partial S(x, z)}{\partial z} \quad (4)$$

The laser source irradiation is given by:

$$I(x) = I_0 \exp \left[ -\left( \frac{x^2}{r_g^2} \right) \right] \quad (5)$$

The term  $r_g$  is the radius of the Gaussian laser beam.

### 3. Numerical Model

The investigation is carried out for a solid composed by an amorphous silicon film layer with thicknesses equal to 0.25  $\mu\text{m}$ , 0.5  $\mu\text{m}$  and 1.0  $\mu\text{m}$  while the thickness of TCO layer and glass substrate is 0.6  $\mu\text{m}$  and 50  $\mu\text{m}$ , respectively. Thermo-physical and optical

properties of the employed materials are reported in tab.1.

Table 1: Thermo-physical properties and refractive index for $\lambda = 1064$ nm of the employed materials			
	k [W/mK]	$\rho c_p$ [J/m <sup>3</sup> K]	$\bar{n} = n - ik_{est}$
glass	1.4	1200	1.46-i 0.0
TCO	$39.6 - 2.09 \times 10^{-2} (T - 273.15) + 4.62 \times 10^{-6} (T - 273.15)^2$	$371 + 0.217 (T - 273.15) + 6640$	$1.95 - 0.002$
a-Si	$1.3 \times 10^{-9} (T - 900)^3 + 1.3 \times 10^{-7} (T - 900)^2 + 10^{-4} (T - 900) + 1.0$	$[(171/T)/685 + 952] 2330$	$3.8 - i [0.0443 + 6.297 \times 10^{-5} (T - 273.15)]$

The laser power is set to 0.3 W and a beam radius of 25  $\mu\text{m}$  is chosen. The irradiation distribution is Gaussian and the heat source moves along x axis from  $x_0 = 0$ . Different constant velocities are considered in order to correspond to Peclet numbers equal to 1.0, 2.0, 3.0, 4.0 and 5.0. It represents the ratio between the convective and diffusive terms along the motion direction.

Four different grid distributions have been tested to ensure that the calculated results are grid independent and three different time step sizes have been investigated. The following configuration has been chosen: the film layer has been subdivided into 150 nodes while the number of nodes in the TCO layer is 100 and 600 for glass substrate. The number of nodes in the axial direction is 200. The grid mesh is structured. The maximum temperature differences of the fields are less than 0.1 percent by doubling the mesh nodes.

In order to analyze the coupled optical-thermal fields an electromagnetic and a thermal model have been developed. This combined problem has been studied by means of Comsol Multiphysics 3.4. It has been necessary to adopt the "In-Plane Waves Application Mode" and an armonic propagation analysis of TE waves has been chosen. The laser beam is orthogonal to the target and the radiative field related to the absorption-reflection-transmission process in the thin film structure is locally one-dimensional and

so, suitable boundary conditions in the electromagnetic model have been applied, as shown in figure 2.

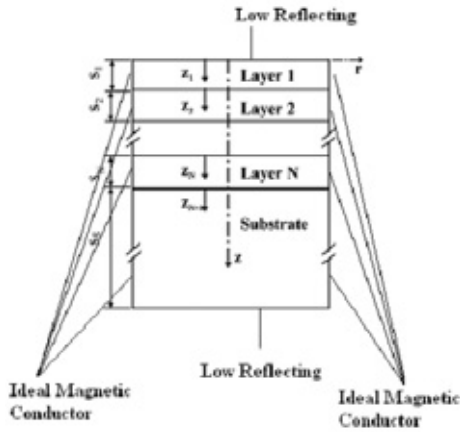


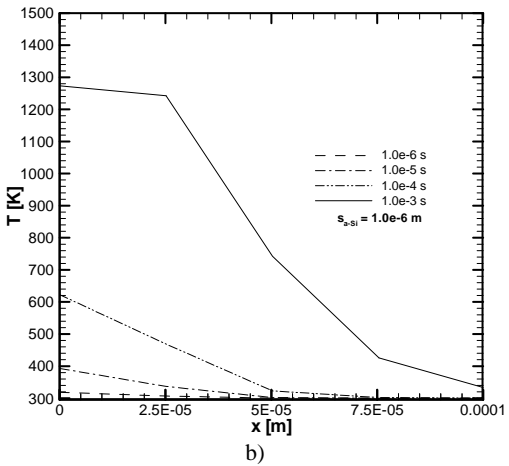
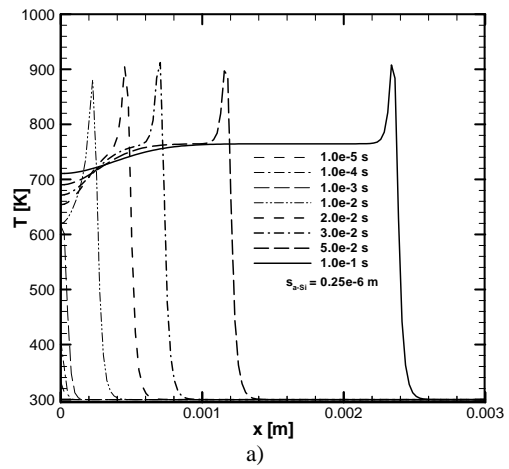
**Figure 2:** Thin film, TCO and glass substrate optical model for front laser treatment.

The two-dimensional heat conduction equation is solved by using the “Heat Transfer Module” and a “Transient analysis” in “General Heat Transfer” window for the thermal model.

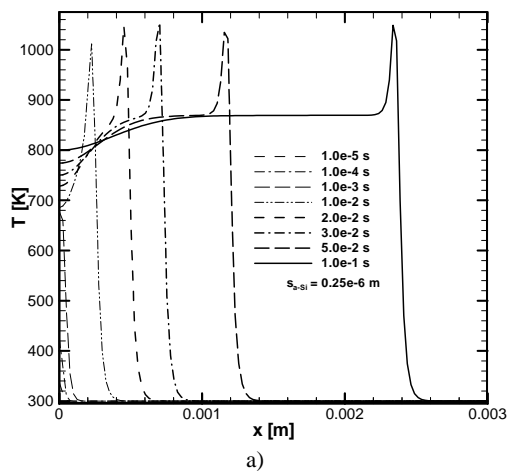
#### 4. Results and Discussion

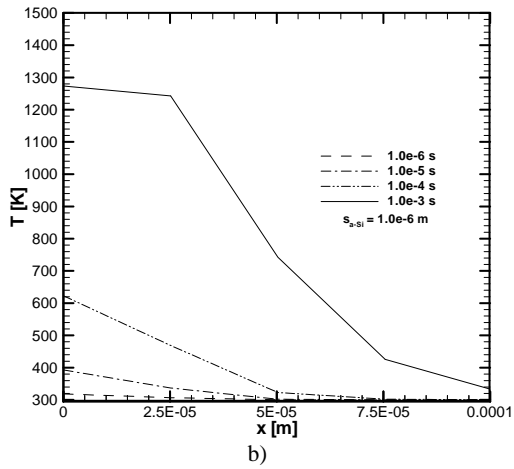
Results related to an amorphous silicon thin films deposited on a TCO layer and a glass substrate, in terms of temperature profiles and fields, are presented in the following.

Figure 3 reports the temperature profiles along x-direction for  $Pe = 1.0$  and  $s_f$  equal to  $0.25$  and  $1.00 \mu\text{m}$ , evaluated at the film surface. It is observed in fig. 3a that the laser spot starts to warm up the zones near the origin. At  $\theta = 1 \times 10^{-3}$  s a maximum temperature equal to  $880$  K is reached and it is localized far from origin. The highest temperature ( $920$  K) is detected at  $\theta = 3 \times 10^{-2}$  s and quasi-steady state condition is reached. When  $s_f$  is equal to  $1.0 \mu\text{m}$  (fig. 3b) the absorbed radiation is larger and, consequently, the temperature and the thermal affected zone are greater; in fact, at  $\theta = 1 \times 10^{-3}$  s temperature attains the value of  $1280$  K and reaches rapidly for the melting point value. For the BT process, as expected, temperature are higher as showed in figure 4; in fact, as reported in figure 4b temperature reaches a value equal to  $1300$  K at  $\theta = 1 \times 10^{-3}$  s.



**Figure 3:** FT - Temperature profiles at surface for  $Pe = 1$  for different times with  $s_f = 0.25 \mu\text{m}$  (a) and  $s_f = 1.00 \mu\text{m}$  (b).

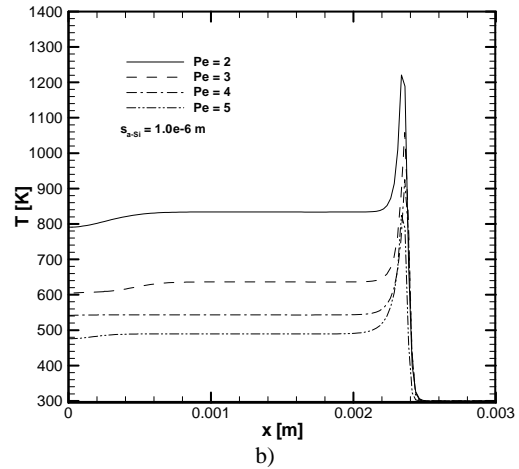
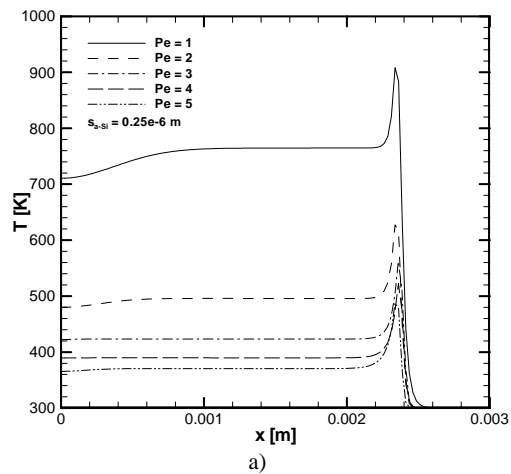




**Figure 4:** BT - Temperature profiles at surface for  $Pe = 1$  for different times with  $s_f = 0.25 \mu\text{m}$  (a) and  $s_f = 1.00 \mu\text{m}$  (b).

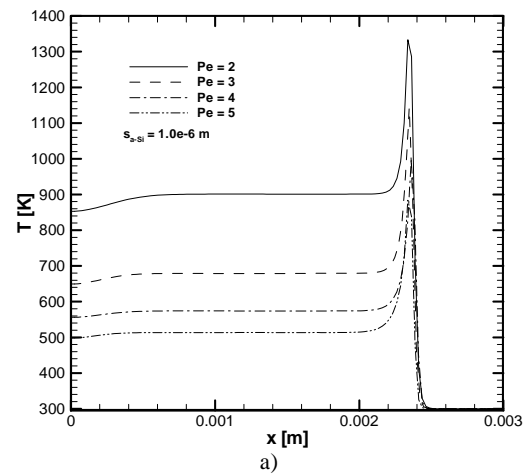
Figures 5 and 6 exhibit a comparison among the temperature profiles along  $x$ -axis for different values of Peclet numbers and film thickness at quasi-steady state condition, such as when the temperature peaks keep constant. It is observed that for both the processes the smaller is the Peclet number and the larger is the film thickness the higher is the attained temperature.

In fact, in fig. 5b it is observed that for  $Pe = 2.0$  and  $s_f = 1.00 \mu\text{m}$ , the temperature peak is equal to 1240 K while for the back treatment process, reported in figure 6b, temperature are 100 K higher at least. Furthermore, asymptotic temperature values raises as  $Pe$  numbers decrease and the zones not irradiated by the spot show more evident diffusion phenomena.



**Figure 5:** FT - Temperature profiles at silicon surface for different Peclet numbers at quasi-steady state condition for  $s_f = 0.25 \mu\text{m}$  (a) and  $s_f = 1.00 \mu\text{m}$  (b).

Figure 7 depicts the temperature profiles along  $z$ -direction at  $x = 0.0025$  m as the steady-state condition has been observed for the front treatment process. Figure 7a refers to  $s_f$  equal to 0.25 and 0.50  $\mu\text{m}$ . The temperature increases linearly along the glass substrate and the diffusive effects are evident in the TCO layer where the temperature is almost constant. Then the temperature grows rapidly and reaches its peak on the surface of the thin film (fig.7a). Fig. 7b exhibits, as previously described, the highest temperatures. For the back treatment process the differences in terms of temperature considering different thin film thicknesses are amplified as reported in figure 8.



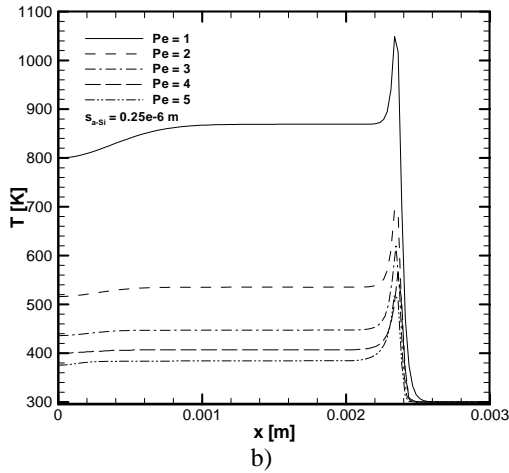


**Figure 6:** BT - Temperature profiles at silicon surface for different Peclet numbers at quasi-steady state condition for  $s_f = 0.25 \mu\text{m}$  (a) and  $s_f = 1.00 \mu\text{m}$  (b).

Temperature peaks are localized near the amorphous silicon surface and in the case of  $s_f$  equal to  $1.0 \mu\text{m}$  temperatures are significant at high Peclet numbers. In fact, as depicted in figure 8b the thin film attains values of temperature equal to 860 K and 940 K, respectively, as  $Pe = 5.0$  and  $4.0$ .

In figure 9 the temperature fields for  $s_f = 0.25 \mu\text{m}$  and  $Pe = 1.0$  and  $5.0$  are reported at two different times for the front and back treatment processes. For the lowest considered Peclet number it is observed the development of the thermal affected zone inside the semi-infinite solid in figure 9a which depicts a front treatment process.

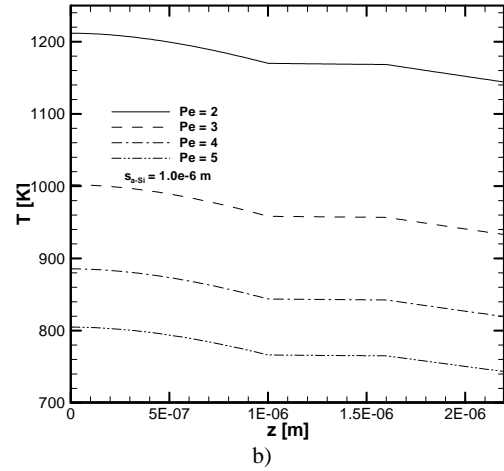
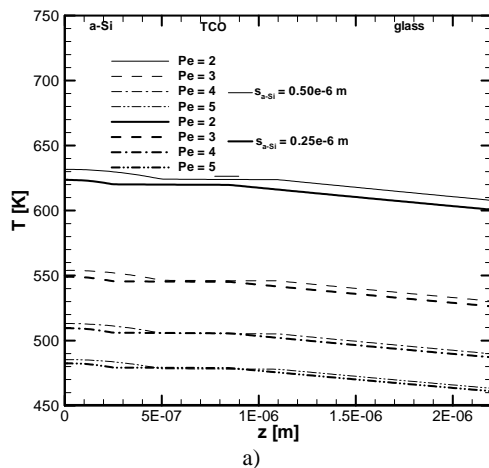


**Figure 7:** FT - Temperature profiles along  $z$ -direction for different Peclet numbers at quasi-steady state condition for  $s_f = 0.25 \mu\text{m}$  and  $0.50 \mu\text{m}$  (a) and  $s_f = 1.00 \mu\text{m}$  (b).

The thin film is almost isotherm whereas the glass substrate presents some temperature gradients. In this zone the heating is due only at the conductive heat transfer because the glass is assumed as a perfect non-absorbent media. The heat affected zone is small but high temperatures are detected on the thin film surface.

In Figure 9b, for  $Pe = 5.0$ , the temperature field shows lower temperature values, greater temperature gradients along  $x$ -axis and a reduced penetration length and less diffusive effects. In the back treatment process it is observed in figure 9c and 9d, higher temperatures, as expected, evaluated on the silicon surface and a larger heat affected zone. Furthermore, the thermal disturb penetrates deeply in the TCO layer and in the glass substrate which attains a temperature equal to about 390 K for  $x < 0.0025$  m.

## 5. Conclusions

A combined optical and thermal fields induced in a multilayer thin film on a glass substrate by a moving laser source was investigated in this paper. The transient two-dimensional analysis was carried out numerically, by means of the COMSOL Multiphysics 3.4 code, for a semi-infinite work-piece along the heat source motion direction. Temperature profiles and fields showed that the maximum temperature values reached within the

structure at the quasi-steady state condition decrease at increasing Peclet number and reducing the film thickness. The transient analysis showed that the time at which the maximum temperature is attained increased with the Peclet number. Higher temperatures and larger heat affected zones are observed for the back treatment processes.

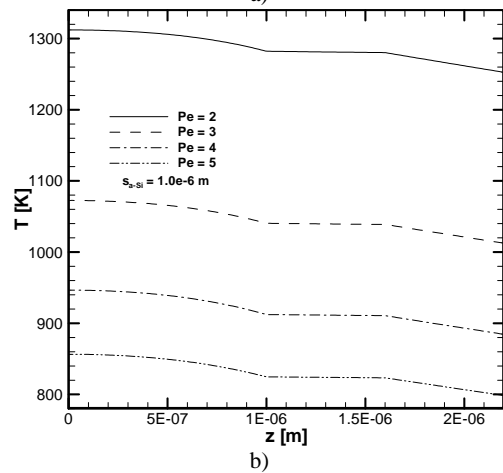
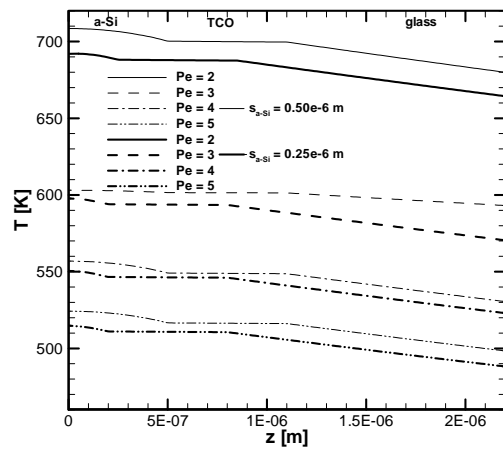
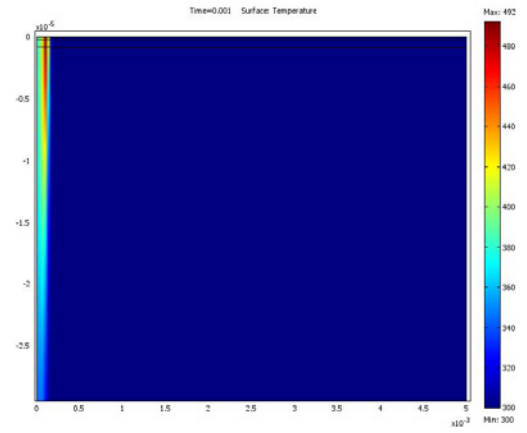
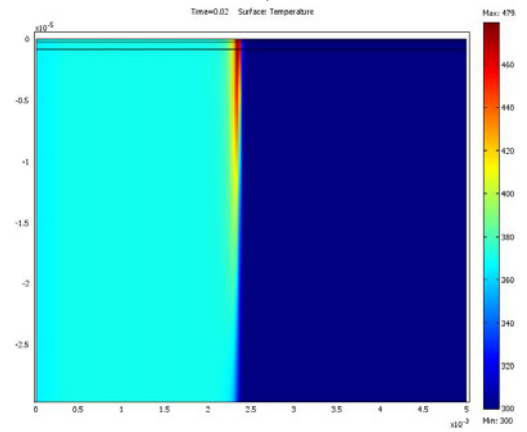


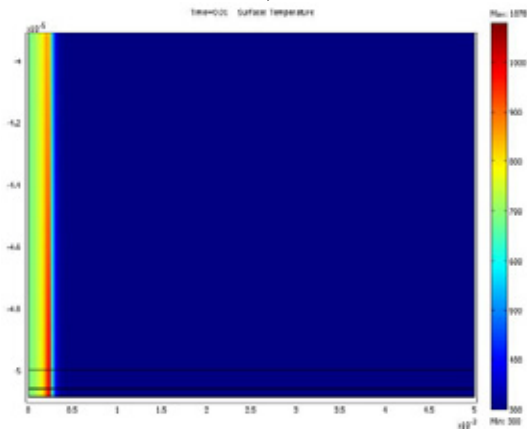
**Figure 8:** BT - Temperature profiles along z-direction for different Peclet numbers at quasi-steady state condition for  $s_f = 0.25 \mu\text{m}$  and  $0.50 \mu\text{m}$  (a) and  $s_f = 1.00 \mu\text{m}$  (b).



a)



b)



c)

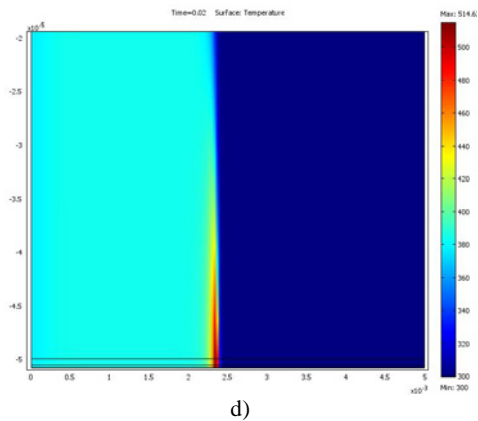


**Figure 9:** - Temperature fields for  $s_f = 0.25 \mu\text{m}$  for  $Pe = 1.0$  at  $\theta = 5 \times 10^{-2} \text{ s}$  (a) and  $Pe = 5.0$   $\theta = 2 \times 10^{-2} \text{ s}$  (b) for a FT process; c) for  $Pe = 1.0$  at  $\theta = 2 \times 10^{-2} \text{ s}$  (c) and  $Pe = 5.0$  at  $\theta = 2 \times 10^{-2} \text{ s}$  (d) for a BT process.

## 6. Nomenclature

$c$  = specific heat,  $\text{J kg}^{-1} \text{K}^{-1}$

$c$  = speed of light,  $\text{m s}^{-1}$

$E$  = electric field,  $\text{N C}^{-1}$

$k$  = thermal conductivity,  $\text{W m}^{-1} \text{K}^{-1}$

$k_{est}$  = extinction coefficient

$n$  = real part of refractive index

$\bar{n}$  = complex refractive index

$Pe$  = Peclet number,  $(v r_g)/(2 \alpha)$ .

$r$  = radius,  $\text{m}$

$T$  = temperature,  $\text{K}$

$u'''$  = generation function,  $\text{W m}^{-3}$

$x, z$  = spatial coordinate

### 6.1 Greek symbols

$\lambda$  = wavelength,  $\text{m}$

$\mu$  = magnetic permeability,  $\text{N s}^2 \text{C}^{-2}$

$\rho$  = density,  $\text{kg m}^{-3}$

$\theta$  = time,  $\text{s}$

### 6.2 Subscripts

$a$  = air

$f$  = film

$g$  = Gaussian

$in$  = initial

$s$  = substrate

$t$  = TCO layer

## 7. References

1. Shah, R. K., Roshan, H. Md., Sastri, M. K. and Padmanahan, K. H., *Thermomechanical*

*Aspect of Manufacturing and Material Processing*, Hemisphere, Washington, DC (1992).

2. Tanasawa, I. and Lior, N., *Heat and Mass Transfer in Material Processing*, Hemisphere, Washington, D.C (1992).

3. Grigoropoulos, C.P., *Heat Transfer in Laser Processing of Thin Films*, Annual Review of Heat Transfer, C. L. Tien ed., CRC, Boca Raton, FL, Vol. 5, Chap. 2, pp. 77-130 (1994).

4. Chen, G. and Tien, C. L., Thermally Induced Optical Nonlinearity During Transient Heating of Thin Films, *ASME J. Heat Transfer*, **116**, pp. 311-316 (1994).

5. McGahan, W. A., and Cole, K. D., Solution of Heat Conduction Equation in Multilayers for Photothermal Deflection Experiments, *J. Appl. Phys.*, **72**, pp. 1362-1373 (1992).

6. Angelucci, N., Bianco, N., Manca, O., Thermal transient analysis of thin film multilayers heated by pulsed laser, *Int. J. Heat and Mass Transfer*, **40**, pp. 4487-4491 (1997).

7. Bianco, N., Manca, O., Two-dimensional transient analysis of absorbing thin film in laser treatments, *ASME Journal of Heat Transfer*, **122**, pp. 113-117 (2000).

8. Nakano, S. et al., Laser Patterning Method for Integrated Type a-Si Solar Cell Submodels, *Jpn. J. Appl. Opt.*, **21**, pp. 1936-1945 (1986).

9. Bianco, N., Manca, O., Ricci, D., A Two Dimensional Numerical Model for Multilayer Thin Films Irradiated by a Moving Laser, *Proc. Comsol Users Conference*, Milano (2006).

10. Bianco, N., Manca, O., Morrone, B., Conjugate Optical-Thermal Model of Back and Front Laser Treatment of Thin Multilayers Films, *Int. Journal of Heat and Technology*, **15**, pp.49-56 (1997).

11. Avagliano, S., Bianco, N., Manca, O., Naso, V., Combined Thermal and Optical Analysis of Laser Back-Scribing for Amorphous-Silicon Photovoltaic Cells Processing, *Int. Journal of Heat and Mass Transfer*, **42**, pp. 645-656 (1999).

12. Bianco, N., Manca, O., Ricci, D., Transient Conjugate Optical-thermal Fields in Thin Films Irradiated by Moving Sources: a Comparison between Back and Front Treatment, European Comsol Conference 2008, Hannover (2008).

13. Rosenthal, D., The Theory of Moving Sources of Heat and its Application to Metal Treatments, *Transf. ASME*, **68**, pp. 849-866 (1946).